Point to point response (in red)

First, we wish to thank the reviewer for urging us to elaborate on the factors that controlled and enhanced the rain centers, and for the valuable advices. Following your review, we used a regional model to further analyze mesoscale processes and inspected the radar and satellite imagery. As you will note, we have gained several new findings, which are specified below and added to the text in red. An additional paragraph lists the factors that explain the high rainfall observed in this storm. We also replaced several parts of Fig. 8 and added 2 new figures.

General comments: The manuscript "Atmospheric Conditions Leading to an Exceptional Fatal Flash Flood in the Negev Desert, Israel" by Uri Dayan et al. deals with a high-impact severe weather situation across Israel. During the slow passage of an unseasonably intense cut-off trough, a three day active weather period was observed what is not typical for this time of the year. Rain was produced by both stratiform and convective processes, with the convective storms in the southern portions yielding the highest impact.

The authors describe the large-scale situation and present backward trajectories that indicate the advection of moist air masses towards Israel. The manuscript improved significantly. However, there are still a few aspects that can be elaborated further.

Following your comments, we added to our analysis "the COSMO regional model (www.cosmo-model.org), operational at the IMS, covering the Eastern Mediterranean domain (25-39E/26-36N, Khain et al., 2020b) with 2.8×2.8 km resolution. The model analyses are created by using a continuous assimilation of the radar and rain gauges composite via latent heat nudging (Stephan et al., 2008, Khain et al., 2020a). The boundary and initial conditions are taken from the European Centre for Medium-Range Weather Forecasts (ECMWF) Integrated Forecasting System (IFS) (www.ecmwf.int/en/forecasts/documentation-and-support). The COSMO model is based on the primitive thermo-hydrodynamic equations that describe non-hydrostatic compressible flow in a moist atmosphere. Its vertical extension reaches 23.5 km (~30 hPa) with 60 model levels, including 12 levels between the surface and 900 hPa and 15 levels between 900 and 500 hPa, being able to capture the PBL effects (Uzan et al., 2020)."

The above description of the model is added as the 4$^{th}$ paragraph of section 2 in our revised manuscript. For more details, see:

http://www.cosmo-model.org/content/model/documentation/core/default.htm

We also further elaborated the radar and satellite imagery to gain the detailed evolution of the major rain centers.

First, the analysis and discussion on the development of instability can be more focused. From the manuscript, the main focus seems to be unseasonable cold mid-level air what is also associated with the intensity of the upper cut-off trough. As strong diurnal heating took place prior to convection initiation, one can argue that this diabatic heating lead to steep lapse rates. In the next step, the overlap of these lapse rates with the rich moisture can be analysed. Finally, indices like CAPE, KI and MKI might be presented to highlight the area of instability.

The warming during the day hours of 26 April 2018 is demonstrated by the 925 hPa temperature. The maps for 07, 09 and 12 UTC (corresponding to 09, 11 and 14 LST) show a

gradual warming during the hours when the sky was clear. The hours 09 and 12 UTC correspond to the beginning of the rain events in Tzafit and Beit Shean, respectively.

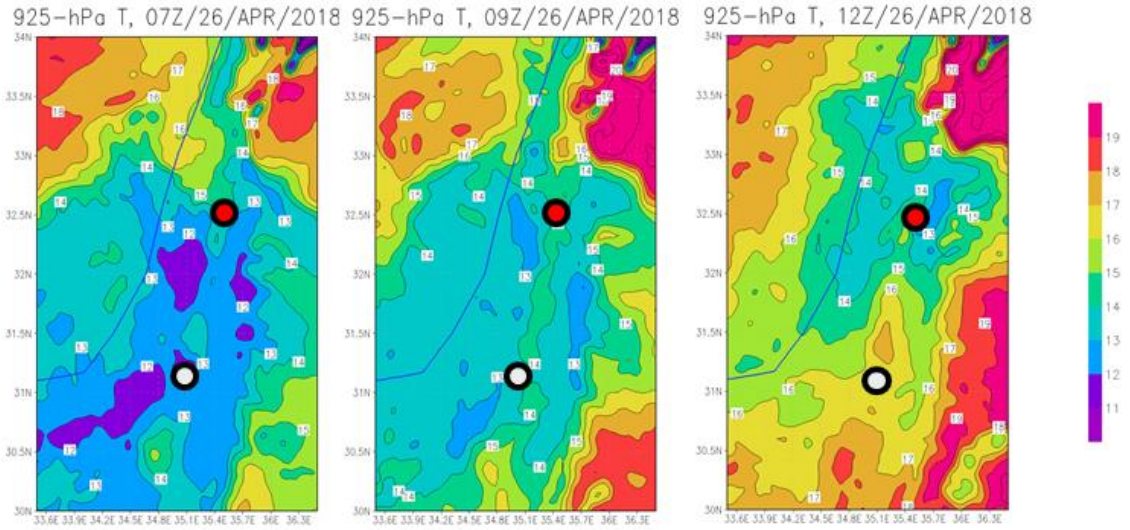


Temperature at 925 hPa for 26 Apr 2018 07, 09 and 12 UTC (left to right). Tzafit is denoted by a white circle and Beit Shean – by a red one.

The spatial distribution of muCAPE (most unstable CAPE) was derived from the COSMO model output, since the only sounding station in Israel is that of Beit Dagan, only twice a day (as is mentioned in the manuscript). The muCAPE shows a general increase during the day hours inland, especially between 10 and 12 UTC (12 and 14 LST). A pronounced maximum, of 1200 J/kg with an elongated shape, is seen north of Tzafit, along the path of the rain producing cells in 09 UTC (north-south, see below), just before the rain started there. This maximum moved eastward, weakened and changed structure later. As for Beit Shean, a buildup of a pronounced muCAPE maximum, of >1500 J/kg, is seen around it in 12 UTC, just before the rain started there.

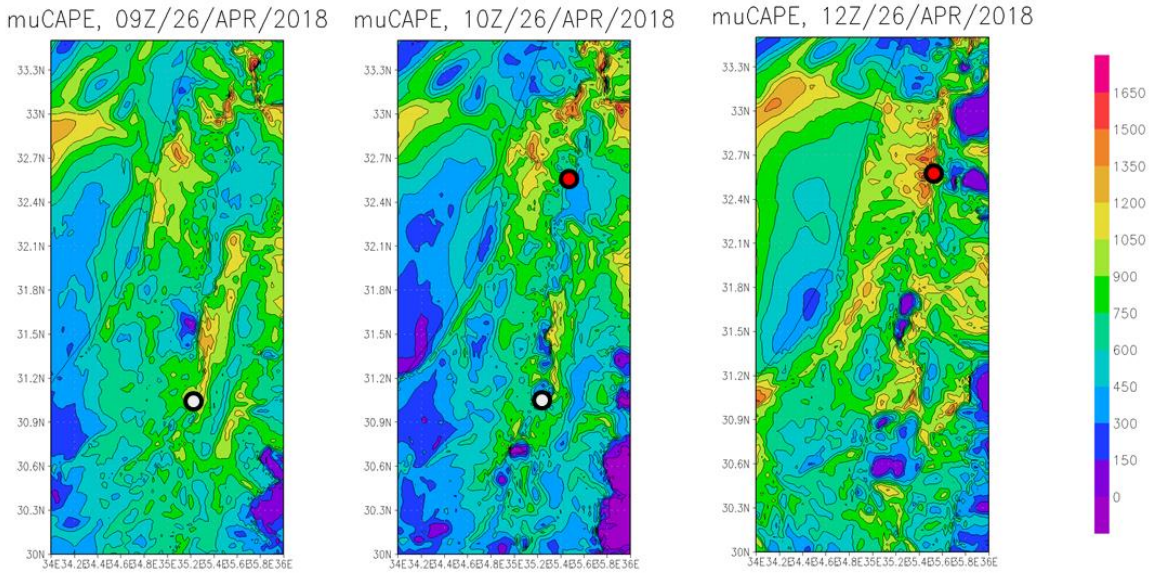


Spatial distribution of muCAPE for 26 Apr 2018 07, 09 and 12 UTC (left to right). Tzafit is denoted by a white circle and Beit Shean by a red one.

The thermodynamic profile derived from the COSMO model at the location of Tzafit for 09 UTC was plotted, and the CAPE and LI were calculated manually, yielding 1075 J/kg and 4.0 K respectively. The respective values for Beit Shean at 12 UTC (prior to the rain there) were 1740 J/kg, and 4.5K, respectively.

The daily warming as a factor for the building up of instability is now mentioned in the abstract and is included in discussion section 4, (lines 368-372), as a part of the 1st in the list of factors that explain the high observed rainfall, as follows: " The considerable rainfall in the three major rain centers described above can be explained by several factors: The high degree of instability, originated by the upper-level cold air, which was further enhanced by the intense solar radiation prior to the three rain events, as implied by the date, latitude and the clear sky (Fig. 8a). This effect is reflected by the MKI maps (Figs. 8g,h), showing much higher values inland compared to these along the coastal region (35°C in Tzafit Basin compared to 13.2°C in Beit Dagan). This is also reflected by a gradual increase in CAPE during the morning hours (not shown), up to 1740 $Jkg^{-1}$ in Beit Shean."

The maximal CAPE value is addressed first in the abstract. CAPE values are also emphasized in Sec. 3.1 (line 238) and in Sec. 3.2 (line 300).

The MKI map for 09 UTC, below, shows high values (>35K) north of Tzafit, where the flood producing rain clouds were formed. The MKI over Judean Mts. and Beit Shean at that time was marginal for intense convection. At 12 UTC, however, just before the rains began in Beit Shean and Judean Mts., the MKI in the 3 locations reached 35°C, i.e., favorable for intense convection.

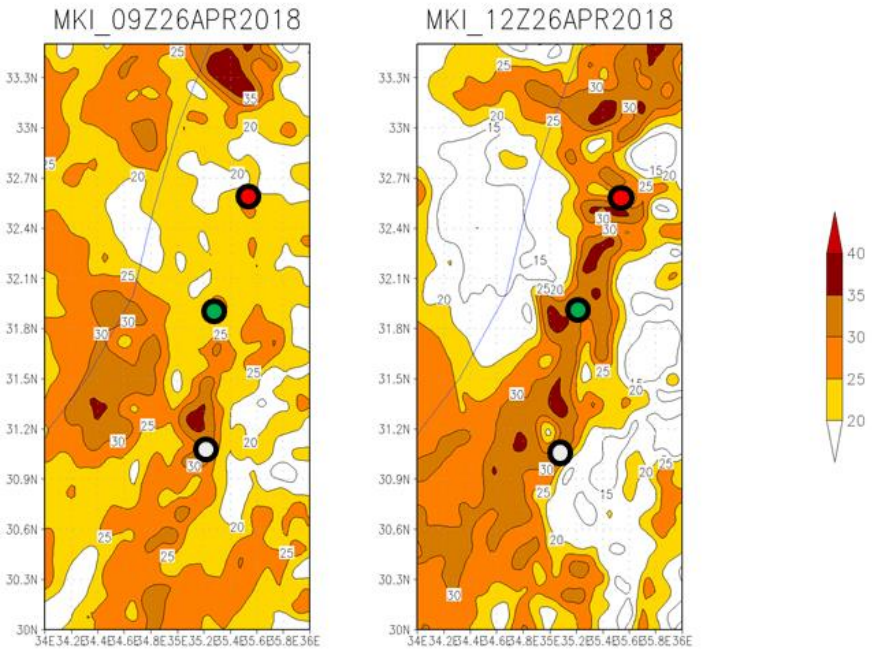


MKI distribution for 26 Apr 2018 09 and 12 UTC. The white and red dots denote Tzafit and Beit Shean, respectively, and the green represents the Judean Mts.

These new MKI maps replace now the previous ones (based on the ERA5 with 30 km resolution data) included in Fig. 8. The values are mentioned in Sec. 3.2 (lines 300-301) and in the discussion on the instability as one in the list of factors explaining the high rainfall in section 4 (lines 369-372).

Following your request, below are the respective KI fields. The distribution is uniform as compared to that of the MKI. The low relative humidity in 700 hPa over the northwestern part of the study region (see RH map to the right) explains the relative low MKI compared to the KI there at 12 UTC. This demonstrates why KI gives false indications for intense convection when the mid-levels are dry (and cause entrainment of dry air into the forming clouds).

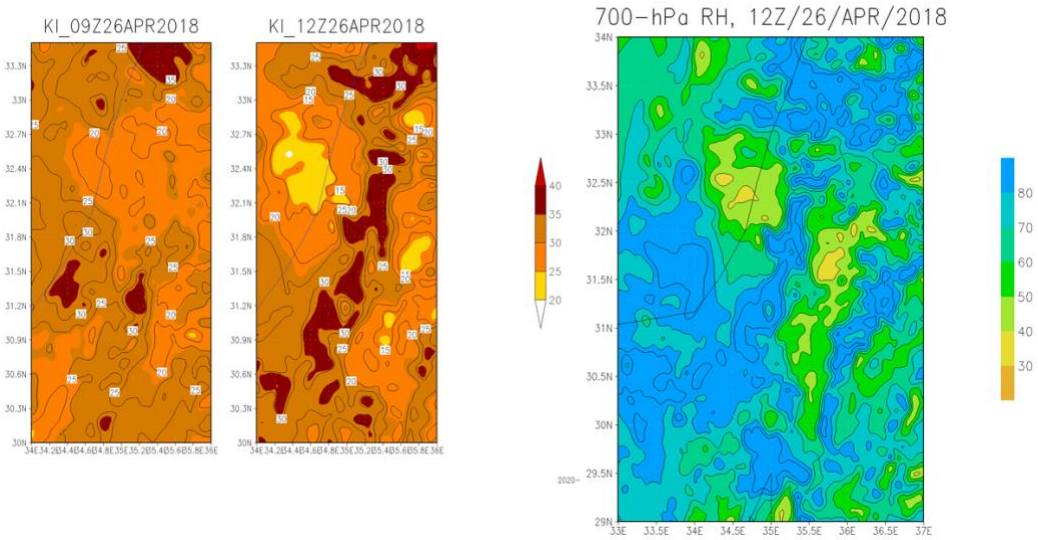


KI distribution for 26 Apr 2018 09 and 12 UTC and relative humidity at 700 hPa for 12 UTC (from left to right). The dots in the KI maps are as in the MKI maps.

Second, lift that causes the storms to initiate needs to be addressed. Mesoscale circulations need to be taken into account and it is important to discuss if baroclinic circulations (fronts, outflow boundaries) were present or not. Then, the influence of the topography can be addressed as already presented (lines 323-324). Are there indications that storms moved along such a boundary where low-level convergence is maximized?

As for mesoscale lifting mechanism for the storm initiation, the vorticity field shown in Fig. 8 of the manuscript (inserted below) reflects two features, which may explain the rains in Tzafit and Beit Shean. The rain in Tzafit can be attributed to a positive vorticity anomaly over the Dead Sea (denoted in blue, north-east of Tzafit), with ~50 km diameter, east of Tzafit (the white point) in 09 UTC. This implies positive vorticity advection via the northeasterly flow at that level. The rain in Beit Shean can be attributed to a pronounced vorticity positive anomaly over the north-west part of Jordan that approached that region (the red point) in 12 UTC from the east.

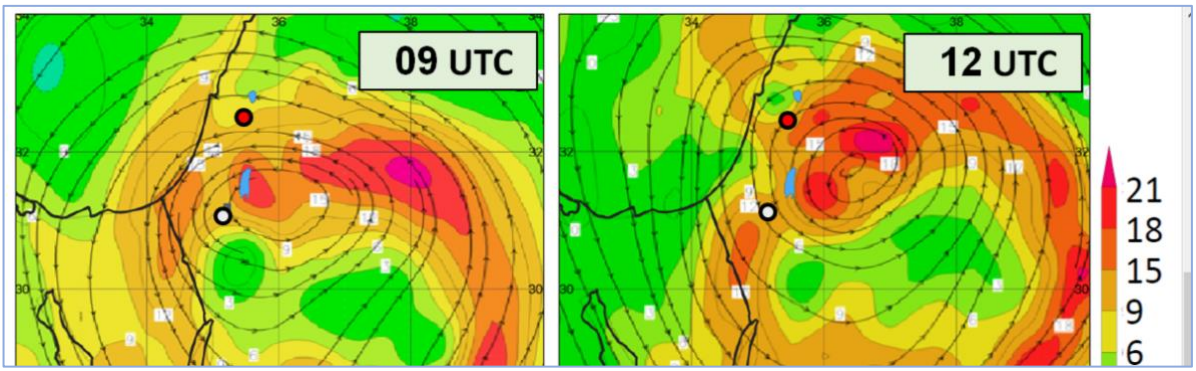


Vorticity and streamlines in 500 hPa, taken from fig. 8 in the manuscript.

The existence of positive vorticity advection is addressed first in section 3.2 in association with the rain in Tzafit in lines 273-275 and in Beit Shean in lines 290-291. This effect is also described in section 4, (lines 335-339) as follows: "Each of these two centres was found to be associated with a positive vorticity advection ahead of a positive anomaly in the 500 hPa level in the ERA5 maps with 30×30 km resolution. The first anomaly was located east of Tzafit at 09 UTC, prior to the rain there (Fig 8e), and the other, east of Beit Shean at 12 UTC, when the rain system started its movement southward over that region (Fig. 8f)."

Concerning the lower levels, for Tzafit, the 925-hPa wind field for 09 UTC, according to the COSMO model (the 1st figure of this document), does not show any specific feature that can indicate a lifting mechanism for the rain there, or north of it. As for Beit Shean, during the rain episode, a lower-level trough extended toward the region from the southeast (Jordan). Its curved shape and orientation (denoted by a blue line) resemble these of the cloud line that caused the rain. This trough and the cloud system that crossed the region southward during that time are shown below, and added to the manuscript, together with a representative radar image, as Fig. 10.

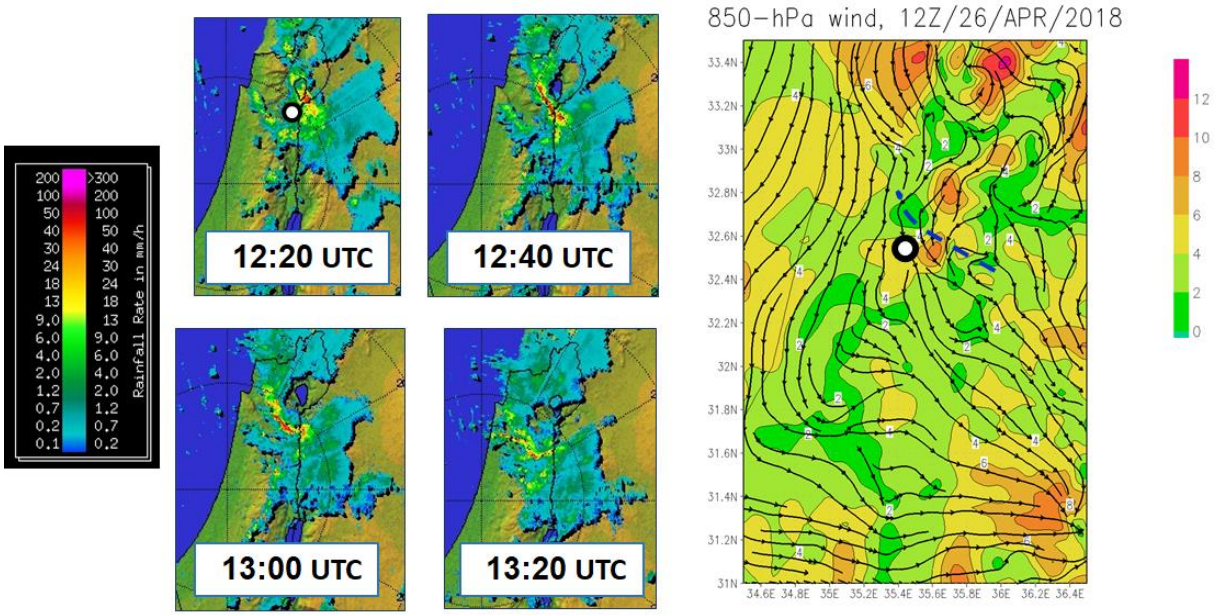


Successive radar images (in mm/h units), in a 20-min intervals, indicating the progression of the precipitative element that crossed Beit Shean (Lake Kinneret is seen northeast of it). Note that the maximum rain intensities reach 50 mm/h. To the right, 850-hPa streamline representing the wind field, with a blue curved line denoting the trough line. Beit Shean is denoted by a white dot in the wind map and in the radar image of 12:20 UTC.

This system is described now in section 3.2 (lines 287-289) as follows: "During this rain episode, a lower-level trough extended toward the region from the southeast (Jordan, Fig. 10c). Its curved shape and orientation (denoted by a blue line) resemble these of the cloud line". It is also mentioned in section 4, in lines 339-341.

Third, next to convection initiation, the potential for storms to produce high amounts of rain needs to be discussed. The amount of rain is dependent on rain intensity (that is also dependent of rain efficiency) and rain duration. From the radar images, it looks like the individual storms were not too large. Given the very localized rain maxima, it may be possible that the slow storm motion contributed to the high rain accumulations. The slow storm motion might be connected to the position of the cut-off trough as the trough center was located over the area of severe storms.

The rain in Tzafit was contributed by several successive cells, 15×15 km on the average, that crossed the region from north to south at an average speed of 12 $ms^{-1}$ (Rinat et al. 2020). This scenario is demonstrated by a series of radar imageries, showing the second cell. The total rainfall for this episode, based on radar echoes, due to lack of rain gauges at the specific, is shown below, having a maximum of 50 mm. These high values can be attributed to the cell propagation vector (train effect), i.e., repeated areas of rain that move over the same region in a relatively short period of time, which may cause flash flooding (e.g., Cordifi et al., 1996).

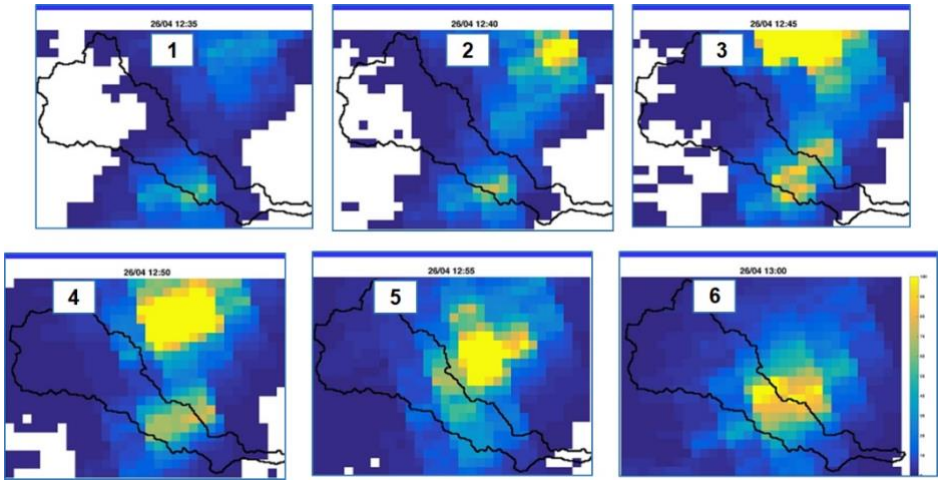


Successive radar images, in a 5-min increments, indicating the progression of a precipitative element crossing the Zafit basin (1 pixel is equivalent to 0.25 $km^2$). The time notations (5 min interval) refer to the summer clock, UTC+3h (with the curtesy of Yair Rinat). The units are mm/h, based on the conversion method of Mara and Morin (2015).

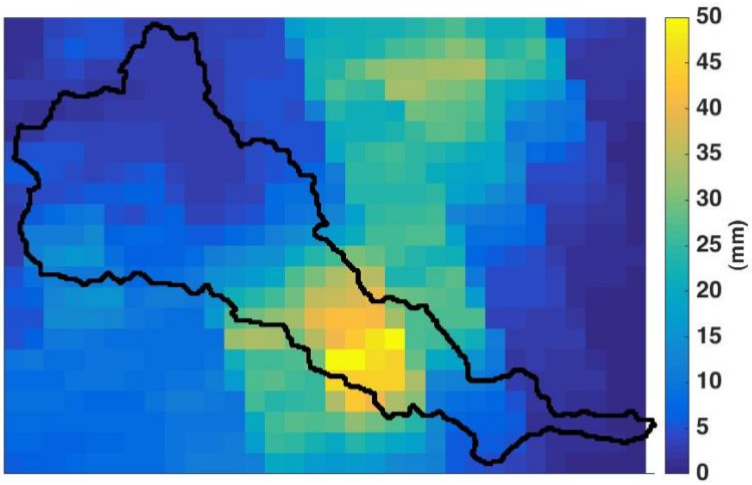


Total rain amount accumulated between 11:40 and 13:40 LST. Note the meridional orientation of the radar images pointing at the "training effect" (with the curtesy of Yair Rinat).

A combination of the two figures above is now added to the manuscript, as Fig. 9. The description of the "train effect" appears in section 3.2, lines 271-273, as follows: ".. evolution is represented by a series of radar images (Fig. 9), showing that it resulted from the passage of several cells that crossed the region from north to south, with an average speed of 12 $ms^{-1}$." It is also included in section 4 (lines 378-380) as factor (e) in explaining the high rainfall in this storm.

As for Beit Shean, here the propagation speed of the rain system was indeed slow (~7 $ms^{-1}$), as can be inferred from the sequence of radar images (above). The rainfall was in the order of 50 mm, with a maximum of 72 mm, presumably contributed by both, the slow movement of the cloud system and the extreme rain intensity (up to 20 mm/h for a 10 min average, Porat et al. 2018). This is noted now in section 3.2, (lines 286-290) and in section 4, (lines 381-382) as the last one in the list of factors explaining the high rainfall in the storm: "The high rainfall in Beit Shean can be partly explained by the slow movement of the rain system, at a speed of 7 $ms^{-1}$."

The rain efficiency can be also discussed, e.g. with respect to limited entrainment given a relatively moist profile (with a history of deep moist convection in the days before) and the vertical distribution of CAPE (i.e. skinny CAPE profiles that allow for slow ascent and much time for the rain production process).

The vertical profiles plotted manually for both Tzafit and Beit Shean indicate that the temperature of the raised air parcels was considerably higher than its surrounding within the medium levels, as reflected by the LI (both exceeding 4K). This implies that slow ascendance was not involved. This and the high CAPE values (>1000 J/kg) indicate that the convection was vigorous.

Moreover, the data can be used to discus the potential for a warm rain process within a deep warm cloud layer, e.g. due to the high temperature at low levels and the rich moisture content at both low- and mid-levels.

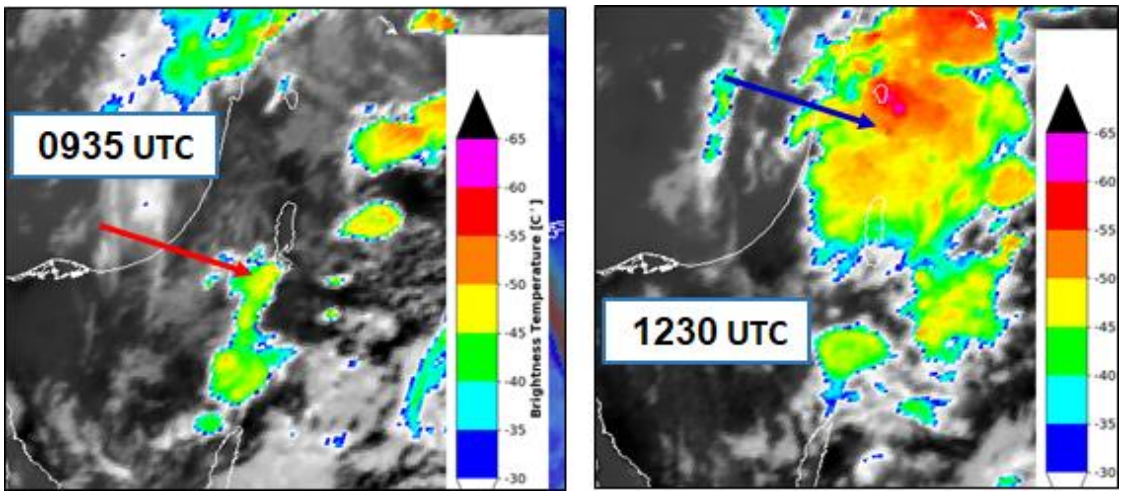


Satellite thermal image for 26 April 2018 (based on METEOSAT IR channel) for the time when the rain attained its maximum intensity (left to right) in Tzafit and Beit Shean (shown by

arrows). The rain clouds over Judean Mts. are seen in the image of 1230 UTC south-west of Beit Shean.

The satellite IR images for the time of the rain in Tzafit and Beit Shean indicate that the cloud tops temperature reached -50°C. The vertical profiles indicate that their elevation exceeded 9000 m, which is 2500 m higher than the average cloud tops characterizing winter thunderstorms in Israel (Altaratz et al. 2001). Since the freezing level during this event was slightly below 3000 m, it can be concluded that the majority of the cloud cells contained a considerable amount of ice particles so that a warm rain process does not seem to be one of the factors for the high intensities observed.

The above METEOSAT satellite images replace now the previous ones in Fig. 8 (a,b). The low top temperatures are mentioned now in section 3.2, (lines 302-304): "… the tops of clouds of the three precipitative centers reached -50°C. According to the temperature profiles over the study region during the storm, this implies that these clouds exceeded 9000 m elevation." This factor is the second in the list of factors that explain the high observed rainfall in section 4 (lines 373-374): "The high elevation of the cloud tops in the three major rain centers, exceeding 9000 m ASL., 2500 m higher than that typifying the tops of the winter thunderclouds in Israel (Altaratz et al., 2001)."

**References**

Altaratz, O., Levin, Z., Yair, Y. 2001: Winter thunderstorms in Israel: A study with lightning location systems and weather radar, Mon. Wea. Rev., 129: 1259-1266.

Corfidi, S. F., J.H. Merritt, and J.M. Fritsch, 1996: Predicting the movement of mesoscale convective complexes. Weather and Forecasting, 11, 41-46.

Marra, F., and Morin, E.: Use of radar QPE for the derivation of Intensity–Duration frequency curves in a range of climatic regimes, Journal of Hydrology 531, 427–440. http://dx.doi.org/10.1016/j.jhydrol. 2015. 08.064, 2015.

Porat, A, Halfon, N and Forshpan A.: Examining the exceptionality of 25-27 April 2018 storm, IMS August (in Hebrew), 2018.

Rinat, Y., Marra, F., Armon, M., Metzger, A., Levy, Y., Khain, P., Vadislavsky, E., Rosensaft, M., and Morin, E., 2020: Hydrometeorological analysis and forecasting of a 3-day flash-flood-triggering desert rainstorm, https://doi.org/10.5194/nhess-2020-189, Preprint. Discussion started: 2 July 2020.